Biomass to chemicals and fuels using advanced thermochemical concepts

Osorio Velasco, Jessi

DOI:
10.33612/diss.843644641

Chapter 3

Sawdust pyrolysis in molten salts using a novel staged free fall reactor

Manuscript in preparation

J. Osorio Velasco, P. Badr, Songbo He, R.H. Venderbosch, H.J. Heeres.

Abstract

Pyrolysis of lignocellulosic biomass is an attractive technology to obtain biofuels and biobased chemicals. Here, we report the pyrolysis of sawdust in a molten salt composed of $ZnCl_2$-KCl-NaCl (44.3:41.9:13.8 mol ratio) using a novel staged free fall pyrolysis set-up. The effect of process conditions were optimised using an experimental design and the highest liquid yield was 71.2 wt %, obtained with 5 wt % biomass in the feed and a pyrolysis temperature of 375 °C. Detailed analyses of the obtained liquid phase revealed the presence of significant amounts of acetic acid, furfural and water. A benchmark experiment without molten salts revealed that the level of depolymerisation of wood is by far lower than for experiments in the presence of salts, indicating a catalytic effect of the molten salt. This study also confirms the suitability of the free fall pyrolysis unit for pyrolysis in molten salts.

3.1. Introduction

Effective biomass transformation through thermochemical routes such as pyrolysis enables the production of biobased chemicals and biofuels. Fast pyrolysis is the rapid heating of the biomass source in an oxygen-free atmosphere resulting in cracking of its constituents (cellulose, hemicellulose and lignin) to lighter compounds that are subsequently condensed to a liquid known as pyrolysis- or bio-oil [1,2]. It is a complex process in which, simultaneously, a large number of physical and chemical phenomena take place. Parameters such as feedstock, temperature, particle size, heating rate, and particle and vapour residence time have an important effect on the product yields [3]. Various pyrolysis technologies have been developed to achieve efficient thermal depolymerization and some have been scaled up to commercial operation [2,4–10].

In recent years, there has been a resurgence in the use of molten salts for biomass pyrolysis. Such salts may offer several benefits, including their ability to liquefy or disperse biomass, thus facilitating feeding, and potentially enhancing liquid yields due to their high thermal conductivity and heat capacity. Typically, eutectic mixtures of various salts, such as $ZnCl_2$, KCl, NaCl, $MgCl_2$, and $CaCl_2$, are employed. These mixtures have lower melting points than the individual salts. Table 3.1 provides examples of molten salt systems explored for lignocellulosic biomass pyrolysis and gasification. In addition to serving as a heating and transport medium, molten salts can also act as catalysts during pyrolysis [11]. Catalytic effects of salts in pyrolysis experiments have been observed previously for thermal pyrolysis in the absence of molten salts. For instance, the minerals present within the biomass such as oxides of Si, Ca, K, Na, and Mg [12] are known to affect the product distribution by catalysing secondary reactions during pyrolysis [13,14]. Further studies in which deliberately minerals were introduced in the biomass feed or removing them from the organic matrix (for example by washing) have proven this effect [15–17]. Reportedly, the catalytic action of molten salts allows a reduction in pyrolysis temperature,

decreasing the energy requirements for the process and better control in reaction selectivities [18,19].

Table 3.1. Molten salts systems used in pyrolysis and gasification of biomass and their respective melting points.

	Components	**Molar ratio**	**Melting point (°C)**	**Ref.**
Carbonates	Na_2CO_3-Li_2CO_3-K_2CO_3	29.8:44.1:26.1	395	[20–22]
	Na_2CO_3-K_2CO_3	54.3:45.7	710	[23]
Halides	$AlCl_3$-KCl	67:33	128	[24]
	$AlCl_3$-NaCl	55:45	133	
	$ZnCl_2$-NaCl	70:30	255	
	$ZnCl_2$-KCl-NaCl	60:20:20	203	
	$ZnCl_2$-KCl-LiCl	40:20:20	240	
	KCl-LiCl-NaCl	36:55:09	346	
	$ZnCl_2$-KCl-CuCl	48.1:41.1:10.8	190	
	$ZnCl_2$	-	283	
	CuCl-KCl	65:35	150	[25]
	$ZnCl_2$-KCl	70:30	262	[26]
	LiF-NaF-KF	46.5:11.5:42	454	[27]
Nitrates/	KNO_3-$NaNO_3$ (Solar salt)	55.8:44.2		[28]
Nitrites	$LiNO_3$-$NaNO_3$-KNO_3	32.8:20.5:46.7	118	[29,30]
	KNO_3-$NaNO_2$-$NaNO_3$	53.1:40.1:6.8	142	[31]
Hydroxides	NaOH	-	318	[32]
	NaOH-KOH	51.15:48.5	170	[33]
Others	NaOH-Na_2CO_3	59:41	284	[34]

An overview of studies using molten salts in biomass pyrolysis is provided in Table 3.2. Typically, the scale of operation ranges from grams up to few kg h^{-1} scale and various salts have been used. Liquid yields of around 35% at 450 °C have been reported using $ZnCl_2$, which is lower than for experiments without molten salts, but

the selectivity to specific compounds is reported to increase. Jiang *et al.* performed pyrolysis experiments with cellulose and rice stalk using a $ZnCl_2$-KCl mixture in a free-fall reactor [25]. The biomass particles were fed into a molten salt bath at temperatures between 410 and 510 °C. The yield of the pyrolysis liquid increased from 14% (78% water) at 450 °C to 21% (40% water) at 530 °C. However, a further increase in temperature resulted in a decline in the liquid yield and an increase in gas yield due to secondary cracking reactions.

Nygård *et al.* investigated the thermal properties of various molten salt mixtures in combination with biomass [27,28]. In their experiments, biomass pellets were submerged in three different molten salt systems (LiF–NaF–KF, Li_2CO_3–Na_2CO_3–K_2CO_3, $ZnCl_2$–KCl) in a temperature range of 400-600 °C. The temperature of the biomass sample was monitored during heating using a thermocouple. Among the systems tested, a mixture of LiF-NaF-KF (FLiNaK) was found to heat up the biomass sample most rapidly (218 °C s^{-1}). The use of nitrate-based salts resulted in a sharp increase in sample temperature above the reactor temperature, suggesting the occurrence of strong exothermic reactions during pyrolysis due to the presence of nitrates. The same authors also studied the pyrolysis of beech wood using FLiNaK and Li_2CO_3–Na_2CO_3–K_2CO_3, and measured the yields of liquid, gas, and char at different temperatures [21]. The highest liquid yield (34.2 wt %, with 60 wt % water content) was achieved at 500 °C using FLiNaK salts. Advantageously, The formation of corrosive HF gas, due to hydrolysis reactions of the molten salt at elevated temperatures was not observed.

Table 3.2. Overview of pyrolysis of lignocellulosic biomass in molten salt systems.

Technology	Feedstock	Biomass intake	wt % biomass on salt	Temperature [°C]	Salt	Liquid yield (wt %)	Water content in liquid (wt %)	Ref.
Free fall reactor	Cellulose	0.5-2 kg h^{-1}	~70%	450-600	$ZnCl_2$	35.0	46.0	[25]
					53.8:46.2 $ZnCl_2$-KCl	11.6	50.0	
					66:34 KCl - CuCl	11.8	21.0	
					49.2:39.8:11 $ZnCl_2$ - KCl - CuCl	12.0	45.0	
					53:40:7 KNO_3 - $NaNO_2$ - $NaNO_3$	0	0	
					49.2:42.2:8.6 $ZnCl_2$-KCl-$FeCl_2$, $ZnCl_2$-KCl	15.0	44.0	
Tubular reactor	Sawdust	~5 g	10%	300-450	65:35 KCl - CuCl	37.2	34.94	[24]
					70:30 $ZnCl_2$ – KCl	52.2	46.46	
					70:30 $ZnCl_2$ - NaCl	53.3	53.58	
					52.9:33.7:13.4 $ZnCl_2$- KCl-NaCl	49.0	43.60	
					24:43:33 KCl- LiCl - NaCl	38.7	25.53	
					40:20:40 $ZnCl_2$ - KCl - LiCl	51.5	49.89	
					45.5:18.2:36.4 $ZnCl_2$- KCl-LiCl	66.5	52.48	
Fixed bed reactor	C. cardunculus L.	200 g h^{-1}	50%	500	60:40 $NaNO_3$ - KNO_3	ND	ND	[35]
Batch reactor	Dry Beech and Pine Wood	~4 g	~0.05 %	500	46.5:11.5:42 LiF – NaF - KF	34.2	60.0	[27]
	Beech wood	20-25 g		475-600	29.2:11.7:59.1LiF-NaF-KF	15-34	20-50	[21]
				450-600	31.7:33.7:34.7 Li_2CO_3-Na_2CO_3-K_2CO_3	~20	60-80	

*wt % salt in biomass

Datta *et al*. investigated the pyrolysis of sawdust, print paper, and newspapers in 13 different molten salts in a horizontal tube reactor [24]. Some salts and particularly those containing $AlCl_3$ and $MgCl_2$ decomposed during pyrolysis and were excluded from further study. Process parameters such as carrier gas flow, biomass particle size, pyrolysis temperature, salt composition, and catalyst effects on liquid yields were examined using sawdust as the biomass source. The $ZnCl_2$-KCl-LiCl salt mixture, adjusted to a molar composition of 5:2:4, exhibited the highest pyrolysis liquid yield, 66.5 wt % on biomass in feed, however, with a considerable amount of water (52.5%). Adjusting the molar composition to 52.9:13.4:33.7 for $ZnCl_2$-KCl-NaCl resulted in a lower pyrolysis liquid yield (52.2%) with less water (43.6%). CuCl-KCl (65:35) yielded a lower liquid yield (37.2 wt %) but with lower water content (34.9%). The composition of the pyrolysis liquids was analysed using GC-MS. The major compounds in the $ZnCl_2$-KCl-LiCl oils were water (52.5 wt %), furfural (17.4 wt %), and acetic acid (26.6 wt %). The use of CuCl-KCl resulted in the formation of formic acid (maximum 7.82 wt %). These findings suggest that pyrolysis in the presence of molten salts significantly alters the composition of the final liquid product compared to conventional pyrolysis, potentially due to catalytic effects and/or differences in operating variables.

Pyrolysis of *C. Cardunculus*, a herbaceous perennial crop native to the Mediterranean, was carried out using a molten nitrate salt (60% $NaNO_3$ + 40% KNO_3) [35]. Experiments were conducted at 500 °C in an electrically heated batch set-up containing 230 g of powdered biomass and molten salt. An automated vibrating system was employed to add the biomass to the hot molten salt at pyrolysis temperature. The mass of the biomass converted to permanent gases increased significantly from 23.7 wt % without molten salt to 89.9 wt % with molten salt. A Solid Phase Adsorption (SPA) method was used to determine the composition of the organics in the pyrolysis liquids. Although the yield of product oil was not specified, the yield of GC-detectable components in the pyrolysis oil obtained through molten

salt pyrolysis was 25% lower than the yield in the absence of salts. Yields of benzene and toluene increased 6.5 and 2.5-fold, respectively (based on relative chromatographic areas). In addition, naphthalene was present in the oil obtained when using molten salts, in contrast to experiments performed without the addition of salts. A sharp temperature increase was observed during pyrolysis due to the occurrence of highly exothermic reactions, consistent with Nygård's findings [27].

The objective of this study was to conduct an extensive investigation to demonstrate the use of a novel free fall pyrolysis reactor for pyrolysis of wood in a molten salt ($ZnCl_2$-KCl-NaCl, 44.3:41.9:13.8 mol ratio), and specifically to study the effects of process conditions on liquid yield and product composition. The approach involved a systematic variation of the ratio between sawdust and molten salt, as well as temperature and quantification and analyses of particularly the liquid products. The resulting yields were modelled using a statistical approach, and the model was used to optimize the liquid and organic yields. Furthermore, we compared the results with those obtained from wood-only pyrolysis, *viz.* pyrolysis in the absence of molten salts.

3.2. Experimental section

3.2.1. Chemicals

Pinewood sawdust (BEMAP-pine nr B03) was supplied by Bemap Houtmeel BV. Relevant properties of the sawdust are presented in Table 3.3. Nitrogen gas was obtained from Linde (> 99.99% purity). Tetrahydrofuran (THF, anhydrous, ≥ 99.9%, with 250 ppm BHT as inhibitor), di-n-butyl ether (DBE) were obtained from Sigma-Aldrich and were all reagent grade (> 99% purity). $ZnCl_2$, NaCl, and KCl (analytical purity > 99%) were purchased from VWR Chemicals (Belgium). Toluene was supplied by Biosolve Chimie.

Table 3.3. Relevant properties of the sawdust used in this study

		Quantity
Moisture (%)		7.9
Elemental composition (wt %)	**C**	47.1
	H	6.0
	N	0.07
	S	0.01
	O (By difference)	46.8
Ash (wt %)		1.9
Particle size (mm)		0.05-0.5

3.2.2. Pyrolysis experiments

All experiments were carried out in a staged free fall pyrolysis unit recently developed by us [36]. The core of the unit consists of a tube made of 316 stainless steel with a diameter of 1 × 0.083 inch. The reactor consists of three zones: i) a biomass/salt pre-treater (Figure 3.1-A), ii) a pyrolysis zone (Figure 3.1-B), and iii) a char collector (Figure 3.1-C). The zones are separated by two ball valves (Figure 3.1-V4 and V6), and the temperature of the zones are independently controlled. Afterwards, the vapour product is condensed in a three-stage condensation-separation system, operated at 1, -20, and -50 °C, respectively. The liquid products are collected and mixed in a glass tube and the non-condensable gaseous products are collected in a gas bag for off-line analyses. N_2 is typically used as the carrier gas at a flow rate of 18 ml min^{-1}.

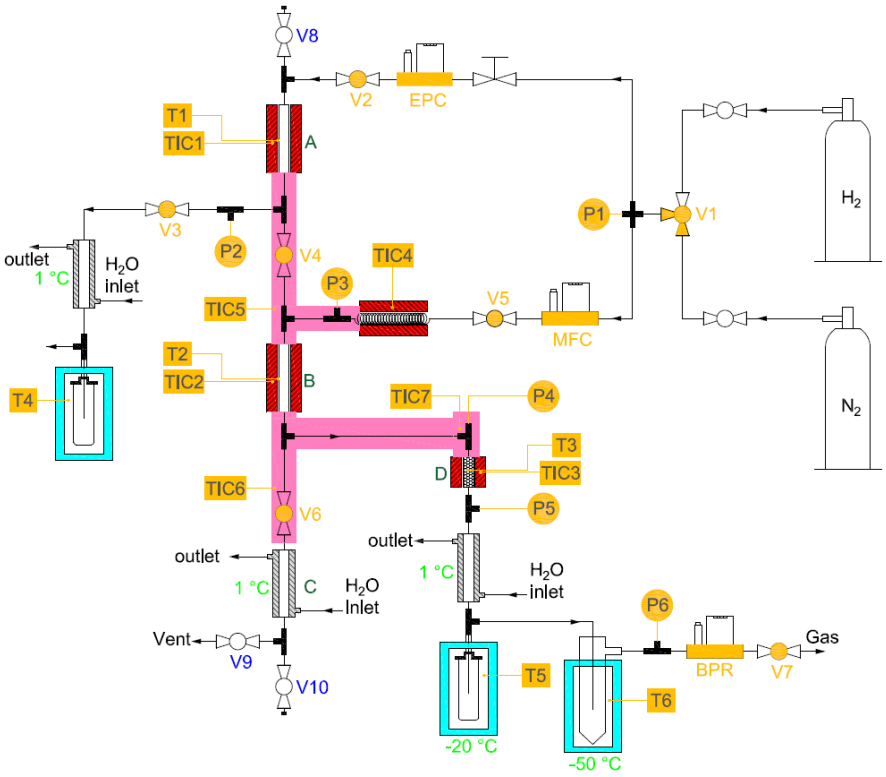

Figure 3.1. Schematic representation of the biomass pyrolysis unit.

To start an experiment, the preheater (A), pyrolysis reactor (B), and zone (D) were heated and maintained at the desired temperatures under a flow of N_2. The temperatures for the three reactors were set at 210 °C, 340-410 °C, and 475 °C, respectively. The desired amount of sawdust/molten salt (7-15 g total) was added to a stainless steel tube (top open, bottom closed) and introduced to the preheater (A) and thermally treated for 10 min to ensure that the salt mixture is melted. The volatiles/moisture were collected in a condenser (Figure 3.1, after V3). Subsequently, the stainless steel tube containing biomass was transferred to the pyrolysis reactor (B) by quickly opening switch V4. Once inside the pyrolysis reactor, V4 is closed and the pyrolysis reaction takes place for a fixed time, typically 20 min for the experiments

described in this paper. The pyrolysis vapours are transferred to zone D, which contains no catalyst in this occasion.

The pyrolysis vapours were condensed in a set of three condensers maintained at 1, -20 and -50˚C, respectively. The liquid products from the condensers were taken, mixed and weighted whereas the non-condensable gases were collected in a Tedlar bag for off-line gas analysis (GC-TCD).

After pyrolysis, the tube containing the solid residue is transported to cooler (C) by gravity by opening V6 and the tube is subsequently removed from the unit. After cooling to room temperature, the solid residue in the tube is weighed for mass balance calculations. In a standard experiment 3 to 5 tubes are injected and the liquid product are collected and mixed. This way sufficient liquid product is obtained to conduct various analyses and experimental errors are minimized.

3.2.3. Determination of product yields

The yields of pyrolysis oil and char in each experiment were measured allowing calculation of the liquid and solid product yield (according to equations 3.1 and 3.2 on a dry sawdust basis). The water content of the liquid was determined using a Karl Fisher titration, allowing calculation of the organics content of the oil. The liquid organic yield is defined in equation 3.3. The yield of the gas phase was determined by difference as it was not possible to accurately measure the weight of the gas phase (equation (3.4)). The feed composition is expressed as the percentage of biomass in the mixture (equation (3.5)).

$$Liquid\ yield\ (wt\ \%\ on\ dry\ biomass\ intake) = \frac{Mass\ of\ liquid\ products\ collected}{Mass\ of\ biomass\ feed} \times 100 \quad \text{(Eq. 3.1)}$$

$$Char\ yield\ (wt\ \%\ on\ dry\ biomass\ intake) = \frac{Mass\ of\ solid\ products\ collected}{Mass\ of\ biomass\ feed} \times 100 \quad \text{(Eq. 3.2)}$$

$$Liquid\ organic\ yield(wt\ \%\ on\ dry\ biomass\ intake) = \frac{Mass\ of\ liquid\ product\ collected - amount\ of\ water\ in\ the\ liquid}{Mass\ of\ biomass\ feed} \quad \text{(Eq. 3.3)}$$

$$Gas\ yield\ (wt\ \%) = 100 - Liquid\ yield - Char\ yield \quad \text{(Eq. 3.4)}$$

$$\%\ biomass\ in\ the\ feed = \frac{Mass\ of\ biomass}{Mass\ of\ biomass + Mass\ of\ salt}\ x\ 100 \quad \text{(Eq. 3.5)}$$

3.2.4. Product analyses

Elemental analyses (C, H, N, and S) for the liquid product were performed using an Euro Vector 3400 CHN-S analyser. Oxygen content was determined by difference. All analyses were carried out in duplicate and the average value is reported.

GC-MS analysis of the liquid products before phase separation was performed using an Hewlett Packard 5973 MS attached to a Hewlett Packard 6890 GC equipped with a Restek Rxi-5Sil MS column (30 m × 0.25 mm × 0.25 µm). The injection volume was 1 µl at an injector temperature 280 °C. The oven temperature was kept at 45 °C for 2 min, raised to 280 °C with a ramping rate of 10 °C min^{-1}, and then kept at 280 °C for 5 minutes.

A Karl Fischer titration was used for the determination of the water content of the liquid phase using a Metrohm Titrino 758 model with Hydranal as the solvent.

The composition of the gas phase was analysed using a GC-TCD Hewlett-Packard 5890 Series II GC equipped with a Poraplot Q Al_2O_3/Na_2SO_4 column and a molecular sieve (5 Å) column. The injector temperature was set at 150 °C and the detector temperature at 90 °C. The oven temperature was kept at 40 °C for 2 min, then heated up to 90 °C at 20 °C min^{-1} and kept at this temperature for 2 min. A reference gas was used to quantify the results (55.19% H_2, 19.70% CH_4, 3.00% CO, 18.10% CO_2, 0.51% ethylene, 1.49% ethane, 0.51% propylene, and 1.5% propane).

3.2.5. Design of experiments

The effects of process parameters for the molten salt pyrolysis of sawdust such as pyrolysis temperature and % biomass in the feed (independent variables) on responses such as liquid yield, organic liquid yield, and char yield were determined. For all experiments, a pre-treatment time of 10 min, a pre-treatment temperature of 210 °C, a pyrolysis time of 20 min and a carrier gas flow of N_2 of 17 ml min^{-1} were applied. A ½ fractional factorial design with two-levels of three factors with three center points and three replicates for corner points was used. A total number of 17 experimental runs were performed and details are given in Table 3.4.

Table 3.4. Experimental results for sawdust pyrolysis in molten salts.

Run	T (°C)[a]	Biomass in the feed (wt %)[a]	Char yield (wt % on biomass)	Liquid yield (wt % on dry biomass)	Liquid organic yield (wt % on dry biomass)
1	375	5	20.6	71.2	4.5
2	400	10	24.5	40.4	6.2
3[b]	375	45	45.2	14.6	3.2
4[b]	375	45	45.8	15.5	3.2
5	350	80	47.9	31.4	12.3
6	340	45	49.3	15.1	3.1
7[b]	375	45	45.8	14.8	3.3
8	375	94	41.0	39.3	18.8
9	410	45	45.8	21.6	4.7
10	350	10	36.9	41.8	5.1
11	400	80	42.7	33.2	14.5
12[b]	375	45	45.9	16.6	3.1
13[b]	375	45	47.7	13.5	2.7
14	400	70	43.2	30.7	14.2
15	400	60	45.3	24.9	8.9
16	400	50	47.3	16.2	6.9
17	400	40	46.6	15.2	3.5

[a]Factors

[b]Center point

The data were analyzed using the Design Expert software package and details are given in the supporting information. A second order regression model (Equation (3.6)) was used to model the responses. A parameter was considered statistically relevant if the P-value is less than 0.050. Backward elimination and elimination of outliers was carried out based on diagnostics to improve the model. The optimum

reaction conditions based on the mathematical model and surface regression graphs were provided by the software.

$$Y_i = \beta_0 + \beta_1 x_{i1} + \beta_2 x_{i2} + \cdots + \beta_k x_{ik} + \beta_{11} x_{i1}^2 + \beta_{22} x_{i2}^2 + \cdots + \beta_{kk} x_{ik}^2 + \beta_{12} x_{i1} x_{i2} + \beta_{13} x_{i1} x_{i3} + \cdots + \beta_{k-1,k} x_{i,k-1} x_{ik} + \epsilon_i \quad \text{(Eq. 3.6)}$$

3.3. Results and discussion

3.3.1. Benchmark pyrolysis experiment

To first assess the reproducibility of experimentation, five experiments were performed using sawdust in molten salts at similar conditions, viz. a relatively low pyrolysis temperature of 375 °C and 45% biomass in the feed. After reaction, a dark liquid was obtained, which separated spontaneously into two liquid phases after a couple of days. All analyses were carried out on the original non-phase separated oil. The liquid yield based on dry biomass intake at this condition ranged from 13.5% to 16.6% with a standard deviation (SD) of 1.1% (Supporting information, Figure S3.11). These results demonstrate a high level of reproducibility for the pyrolysis experiments conducted in the novel pyrolysis unit. This is also confirmed by comparing the solid product yields, which ranged from 45.2% to 47.7% with a SD of 0.9%. The amount of organics in the liquid phase was only limited at these non-optimised conditions and ranged between 18.9 and 22.1 wt % on dry biomass intake, the remainder being water

Effect of salts

To assess the impact of salt on product yields, an experiment was performed in the absence of salt at otherwise similar conditions as for the benchmark experiment described above. The presence of molten salts results in an increase in the gas yield

and a decrease in liquid and solid, see Figure 3.2 for details which is attributed to the catalytic effects of salts promoting depolymerisation reactions. These observations align with literature findings (Table 3.2) It should be stressed that the actual values reported in the Figure 3.2 are far from optimal and by far better results regarding liquid yields have been obtained using molten salts (*vide infra*). The yields for sawdust only (no salts) are also far from optimal, and optimization studies in the staged pyrolysis set-up have led to liquid yields of up to 63 wt % on biomass at much higher temperatures (475 instead of 375 °C) [37].

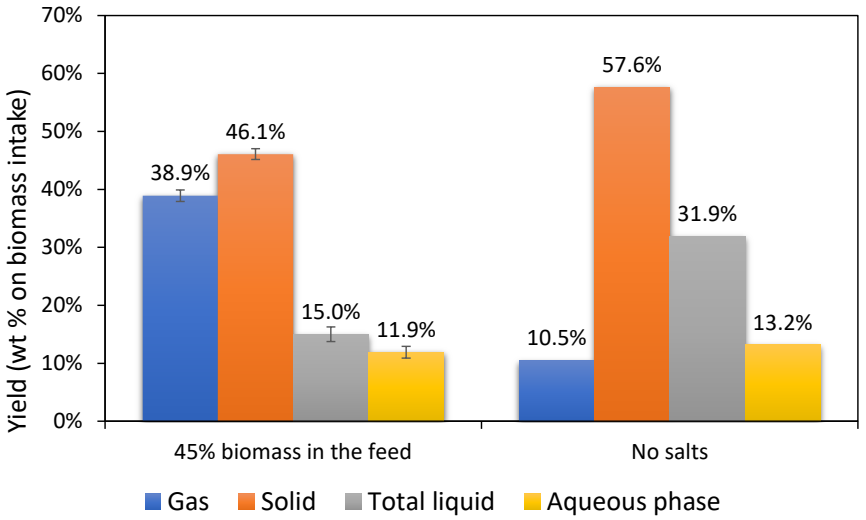

Figure 3.2. Pyrolysis of sawdust with and without molten salts 375 °C, 20 min residence time, 17 ml min^{-1} N_2 flow.

3.3.2. Systematic studies on the pyrolysis of pinewood sawdust in molten salts

Optimization experiments with the objective to obtain high liquid yields with a high content of organics were performed using a design of experiments approach. The experiments were conducted using pinewood sawdust and a eutectic mixture of

$ZnCl_2$:KCl:NaCl (molar ratio of 44.3:41.9:13.8). Different amounts of biomass in the feed were tested, though the total amount of feed was kept constant at 6 g per feed tube. In addition, the pyrolysis temperature was varied between 340 and 410 °C. The latter is determined by relevant properties of the molten salt used in this study, which is known to be hydrolytically stable till this temperature level [38]. A summary of the independent, including the ranges and dependent variables is given in Table 3.5. The individual conditions for the 17 experiments performed are outlined in Table 3.4.

Table 3.5. Summary of the design of experiments.

Independent variables	Pyrolysis temperature	340-410 °C
	% Biomass in the feed	10-100
Output variables (wt % on dry biomass)	Liquid yield	13.5-71.2
	Liquid organic yield	2.7-18.8
	Char	20.6-49.3%
Constant parameters	Carrier gas	N_2
		17 ml min^{-1}
	Pre-treatment	10 min,
		210 °C
	Reaction time	20 min
	Condensation train	5, -20, -50 °C

Liquid yields

The liquid yields within the experimental design window varied considerably and were between 13.5 and 71.2 wt % on dry biomass intake (Table 3.4). The highest liquid yield was obtained at 375 °C and a 5 wt % biomass in the feed. This value is

higher than values reported for wood pyrolysis in molten salts in the literature (Table 3.2). The experimental data were modelled and the ANOVA for the model is given in Table 3.6. The best model is given in equation 3.7, with A representing the temperature in °C and B the wt % biomass in the feed.

$$Liquid\ yield\ (wt\ \%) = 13.36 + 2.46A - 15.64B + 3.04AB + 4.41A^2 + 38.78B^2 + 37.37A^2B \quad \text{(Eq. 3.7)}$$

The R-squared value for this model is > 0.96, indicating that it is a good description of the experimental data. This is also confirmed by a parity plot given in Figure 3.3. The p-value of the model and most of the terms involving the amount biomass in the feed in the model are less than 0.0002, suggesting statistical significance. The VIF value of most of the terms is less than 2.6, indicating a limited correlation between the terms.

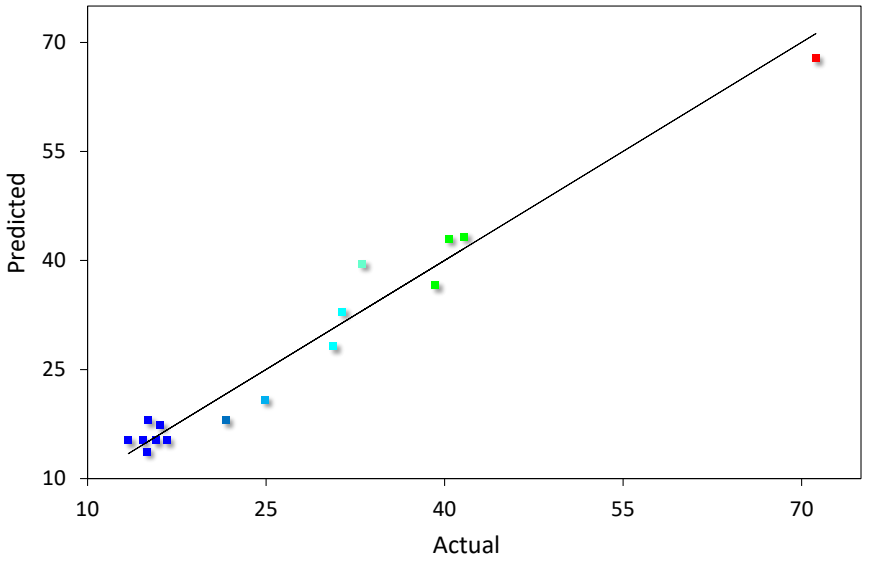

Figure 3.3. Parity plot for the liquid yield (wt % on dry biomass).

The effect of the independent process variables on the product yield is visualised in Figure 3.4. The liquid yield shows a complex relation with both the temperature and the biomass amount in the feed. Two regions were identified where high liquid yield can be achieved *viz.* 1) a low biomass amount in the feed (< 5 wt %), and 2) a high amount of biomass in the feed (> 90 wt %). Between these extremes, the liquid yield is by far lower. These findings are of interest and suggest different actions of salts. In region 1, the salt is present in low amounts and most likely is catalytically active. In contrast, in region 2, the salt is present in large excess and it is well possible that higher liquid yields are attainable in this region by dissolution of the wood, potentially avoiding mass and heat transfer issues as evident for ordinary wood pyrolysis, that typically reduce liquid yields. In the intermediate range, gas phase formation appears to be pronounced, leading to lower liquid yields.

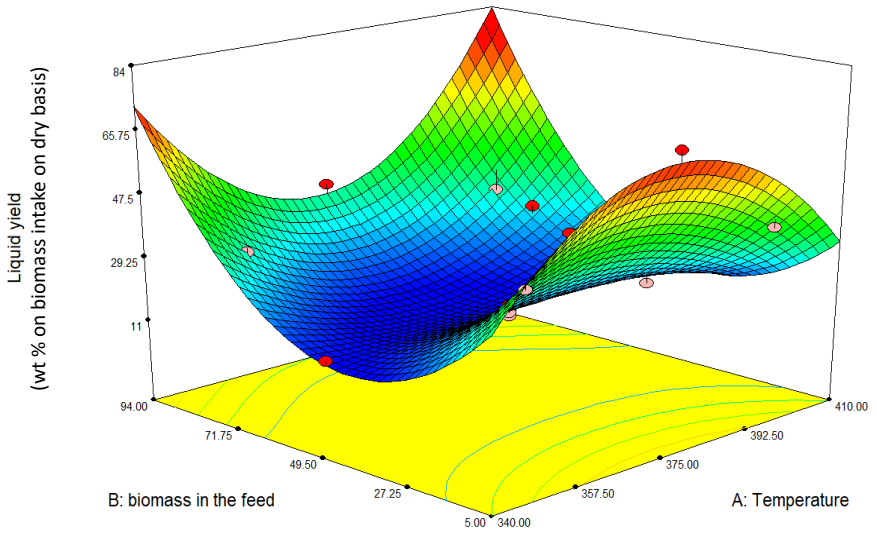

Figure 3.4. Liquid yield Effect of wt % biomass in feed and temperature (°C) on the liquid yield.

Table 3.6. Model results for liquid yield, liquid organic yield and char yield.

Source	Liquid yield (wt % on dry biomass)		Liquid organic yield (wt % on dry biomass)		Char Yield (wt % on dry biomass)	
	R^2	0.9674	R^2	0.9896	R^2	0.9826
Model	VIF	p-value	VIF	p-value	VIF	p-value
		<0.0001		<0.0001		<0.0001
A-Temperature	1.06	0.1357	1.11	0.0024	1.87	0.1585
B-Biomass %	2.43	<0.0001	69.30	<0.0001	10.69	0.9734
AB	1.02	0.3220	1.10	0.2629	1.19	0.3564
A^2	1.09	0.1249	1.75	0.2135	1.08	0.0299
B^2	1.10	<0.0001	2.11	<0.0001	1.18	<0.0001
A^2B	2.57	0.0002	10.12	0.0029	1.94	0.0050
B^3			42.81	0.0007	10.90	0.0049

The influence of temperature on liquid yield is different for region 1 and 2. In region 1, the extremes with respect to temperature appear to be favoured, whereas an intermediate temperature is best in region 2. So far, we do not have a sound explanation for these trends.

Liquid organic yields

As stated earlier, the liquid products obtained after pyrolysis contains significant amounts of water. As such, it is of interest to consider the organic fraction in the liquid, which was obtained indirectly by measuring the water content of the liquid by a Karl-Fischer titration. The organic liquid content (wt % on dry biomass) varied between 2.7 and 18.8 wt %. Best results were obtained at 375 °C and 96 wt % biomass on feed. The experimental data were modelled and the ANOVA for the model is given in Table 3.6. The best model is given in equation 3.8, with A representing the temperature and B the wt % biomass in the feed.

$$Organic\ liquid\ yield\ (wt\ \%) = 5.14 + 1.35A + 19.76B + 0.73AB - 0.30A^2 + 6.29B^2 - 10.25A^2B - 12.56B^3 \quad \text{(Eq. 3.8)}$$

The R-squared value for this model is > 0.98, indicating that it is a very good description of the experimental data. This is also confirmed by the parity plot given in Figure 3.5. The p-value of the model and most of the terms considered in the model are less than 0.05, suggesting that they are statistically significant. The VIF value of most of the terms related with temperature are less than 2.1, indicating limited correlation between the terms. However the VIF values for the terms related with the biomass in the feed are larger than 10, indicating correlation between the terms.

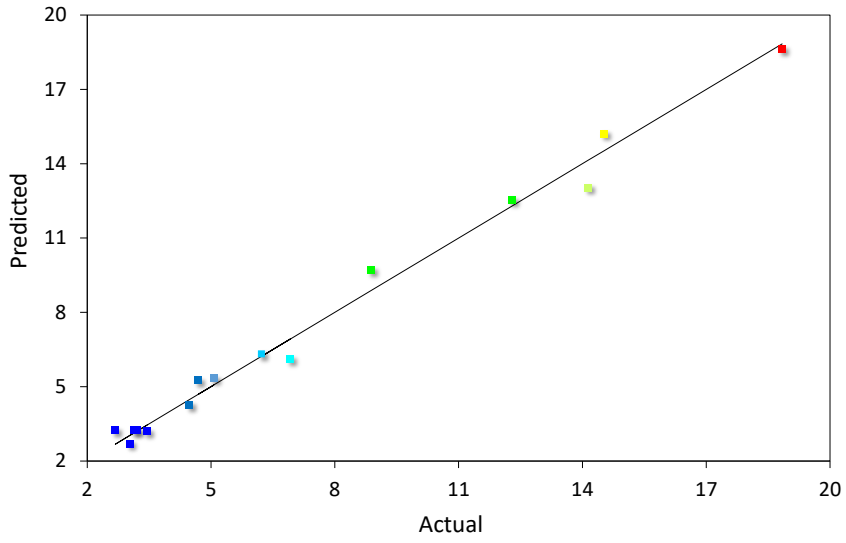

Figure 3.5. Parity plot for the liquid organic yield (wt % on biomass feed).

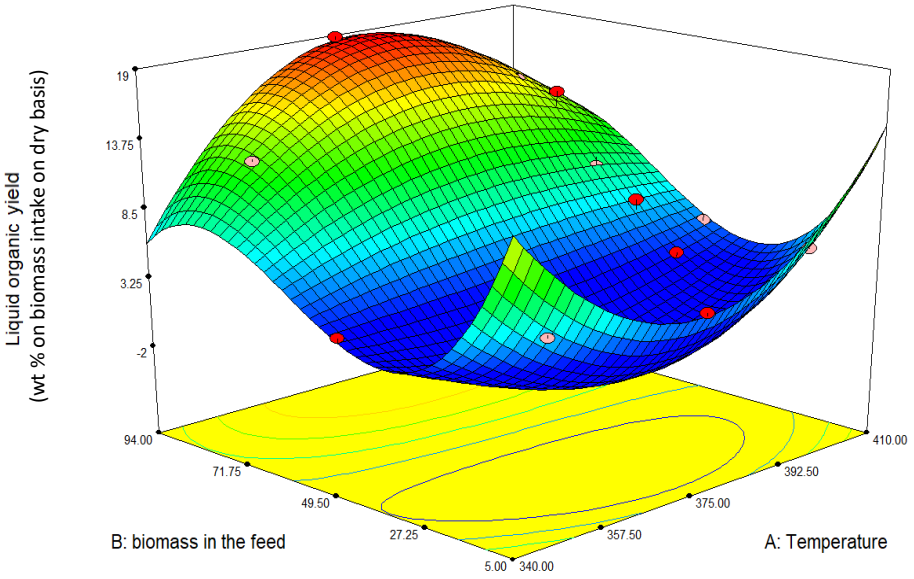

Figure 3.6. Effect of biomass in the feed (wt %) and temperature on the liquid organic yield

The effect of the pyrolysis temperature and the biomass amount in the feed on the liquid organic yield is provided in Figure 3.6. Similar to the liquid yield, two distinct regions are present to obtain high liquid organic yields, *viz.* a region with low amount of salts (region 1) and a region with high amount of salts (region 2). However, in contrast to the liquid yield trends, it is evident that region 1 is favoured and that the use of a small amount of salt is highly advantageous. It implies that higher amounts of salts are catalytically too active, leading to a high production of permanent gases.

Char yields

The char yield was measured independently and, when aiming for high liquid yields, should be minimised. The char yield varied between 20.6 and 49.3 wt % on dry biomass intake (Table 3.4). The highest amount were obtained at low temperatures in the range (340 °C and an intermediate biomass amount in the feed, 45%). The lowest yield, 20.6%, resulted from very low biomass intake of 5%, and a pyrolysis temperature of 375 °C. The best model is given in Equation 3.9, with A representing the temperature and B the wt % biomass in the feed.

$$Char\ yield\ (wt\ \%) = 46.18 - 1.26A + 0.072B + 1.25AB + 2.76A^2 - 14.09B^2 - 7.77AB^2 + 9.74B^3 \quad \text{(Eq. 3.9)}$$

Figure 3.7 provides the modelled relation between temperature, biomass in the feed, and char yield. It implies that temperature is very important and has a major impact on char yield, whereas the biomass amount in the feed is statistically less relevant. The lowest solid yields are obtained at the highest temperatures in the range (400 °C). Thus, when aiming for low char yields, higher temperatures are favoured. However, this not necessarily leads to the desired higher liquid yields (see Figure 3.7)

as gas phase formation is also a function of the temperature and also tends to be favoured at higher temperatures.

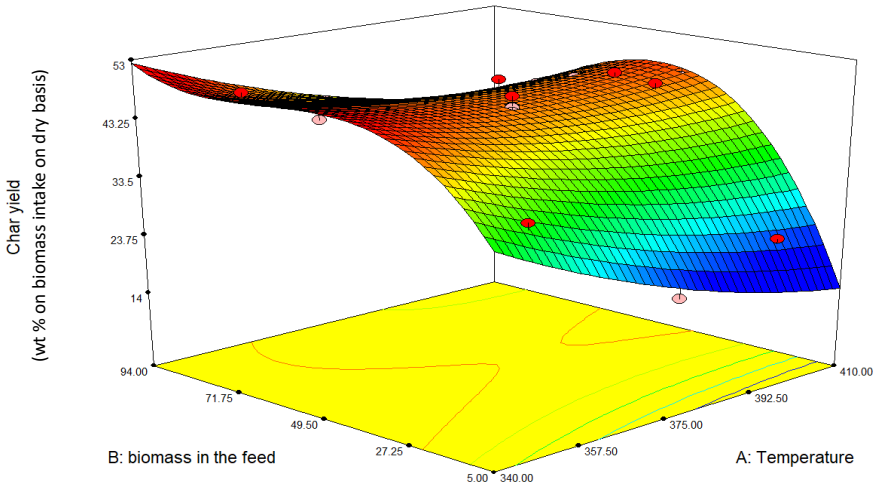

Figure 3.7. The influence of amount of biomass in the feed (wt %) and temperature on the char yield (experimental conditions are given in Table 3.5. Char yield is based on biomass intake (wt %) on a dry basis).

Composition of the liquid phase

A prime objective is to obtain a high liquid yield which preferably contains a large amount of organic platform chemicals. As such, the pyrolysis liquids were analysed using GC-MS, to gain detailed insights into their chemical composition. Relevant GC-MS chromatograms of products obtained with different amounts of biomass in the feed at 400 °C pyrolysis temperature are presented in Figure 3.9 and tables with individual components are provided in the supporting information (Table S3.4 and S3.5). The chromatograms in the absence of salts shows the typical components present in pyrolysis liquids arising from the cellulose and hemicellulose (*e.g.*, hydroxyacetone) and lignin (*e.g.*, phenolics) in the original wood. When the amount

of salts in the biomass is increased, the number of components reduces and at < 70% biomass in the feed, only two major components are present: furfural and acetic acid. The presence of the former was also confirmed by HPLC. These findings are in line with literature data [39,40].

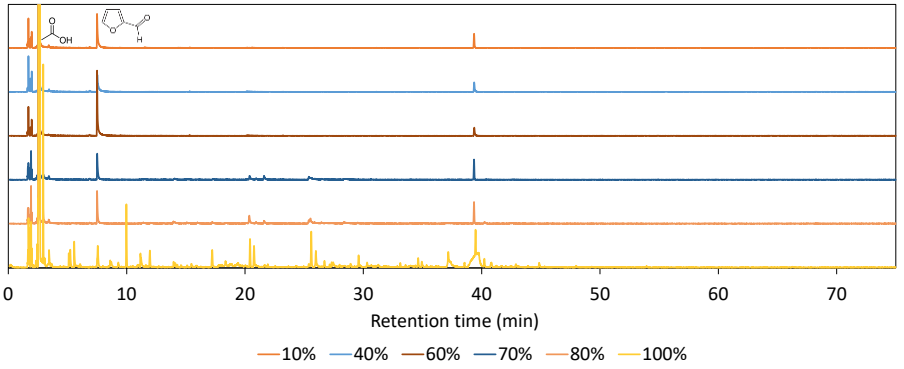

Figure 3.8. GC-MS chromatograms for the liquid product at different % of biomass in the feed at 400 °C (peak at about 40 min is the stabiliser BHT in the solvent THF).

Composition of the gas phase

Although the gas phase could not be quantified in detail, its composition was determined using GC-TCD and the results are given in the supporting information (Figure S3.2). The main components are CO_2 and CO, and to a lesser extent small hydrocarbons like methane, ethane, ethene and propane. The relative amounts differ and are depending on the biomass intake in the feed.

3.4. Conclusions

We have systematically investigated the pyrolysis of sawdust in molten salts in a newly developed free falling pyrolysis reactor. A representative molten salt was used, namely the eutectic mixture of $ZnCl_2$-KCl-NaCl in a molar ratio of 44.3:41.9:13.8. The results revealed that the amounts of molten salts in the feed significantly influence

the product yields. The highest liquid yield of 71 wt % on dry biomass intake was obtained at 375 °C and with 5 wt % biomass in the feed. This yield is higher than reported in literature. Statistical modelling of the data revealed that high liquid yields are a strong function of the amount of biomass in the feed. Two distinct regions for high yields are identified, a region with a low amount of biomass (< 5 wt %), and a region with high amount of biomass (> 90 wt %) in the feed, with lower values at intermediate biomass intakes. These findings seem to imply that the action of the molten salts is a delicate balance between chemical action (*e.g.*, catalysis by the salts), and physical features like mass/heat transfer (biomass particles versus a homogeneous liquefied feed). The highest liquid organic yield was 19 wt %, obtained at 375 °C and 96 wt % biomass in the feed. It was observed that the liquid products contain higher amounts of water compared to thermal pyrolysis under similar conditions. In addition, a lower number of individual monomeric components was detected, the main ones being acetic acid and furfural, indicating the catalytic activity of the salts. Such furfural-rich liquids can serve as valuable precursors for bio-based chemicals using catalytic approaches. In addition, this study also demonstrates the broad applicability of the novel staged free fall reactor for pyrolysis studies.

3.5. References

[1] A.V. Bridgwater, Renewable fuels and chemicals by thermal processing of biomass, Chem. Eng. J. 91 (2003) 87–102. https://doi.org/10.1016/S1385-8947(02)00142-0.

[2] P. Basu, Biomass gasification and pyrolysis: Practical design and theory, Elsevier Inc, Burlington, MA, 2010. https://doi.org/10.1016/C2009-0-20099-7.

[3] A.V. Bridgwater, G.V.C. Peacocke, Fast pyrolysis processes for biomass, Renew. Sustain. Energy Rev. 4 (2000) 1–73. https://doi.org/http://dx.doi.org/10.1016/S1364-0321(99)00007-6.

[4] D. Meier, A.V. Bridgwater, S. Czernik, J.M. Diebold, D. Oasmaa, A. Fast Pyrolysis of Biomass: A Handbook, CPL Press, Newbury, UK, 2008.

[5] M. Ringer, V. Putsche, J. Scahill, Large – scale pyrolisis oil production: A technology Assessment and Economic Analysis, 2006. https://doi.org/NREL/TP – 510-37779.

[6] R.H. Venderbosch, W. Prins, Fast pyrolysis technology development, Biofuels, Bioprod. Biorefining. 4 (2010) 178–208. https://doi.org/10.1002/bbb.205.

[7] BTG bioliquids, Empyro Hengelo, NL - BTG Bioliquids, (2015). https://www.btg-bioliquids.com/plant/empyro-hengelo/ (accessed March 27, 2021).

[8] W. Cai, R. Liu, Performance of a commercial-scale biomass fast pyrolysis plant for bio-oil production, Fuel. 182 (2016) 677–686. https://doi.org/10.1016/j.fuel.2016.06.030.

[9] A.V. Bridgwater, J.M. Double, Production costs of liquid fuels from biomass, Fuel. 70 (1991) 1209–1224. https://doi.org/http://dx.doi.org/10.1016/0016-2361(91)90242-3.

[10] A.V. Bridgwater, Review of fast pyrolysis of biomass and product upgrading, Biomass and Bioenergy. 38 (2012) 68–94. https://doi.org/10.1016/j.biombioe.2011.01.048.

[11] Y. Li, X. Xu, X. Wang, P. Li, Q. Hao, B. Xiao, Survey and evaluation of equations for thermophysical properties of binary/ternary eutectic salts from NaCl, KCl, MgCl2, CaCl2, ZnCl2 for heat transfer and thermal storage fluids in CSP, Sol. Energy. 152 (2017) 57–79. https://doi.org/10.1016/j.solener.2017.03.019.

[12] J. Akhtar, N. Saidina Amin, A review on operating parameters for optimum liquid oil yield in biomass pyrolysis, Renew. Sustain. Energy Rev. 16 (2012) 5101–5109. https://doi.org/10.1016/j.rser.2012.05.033.

[13] Q. Lu, Y. Zhang, Z. Tang, W. Li, X. Zhu, Catalytic upgrading of biomass fast pyrolysis vapors with titania and zirconia/titania based catalysts, Fuel. 89 (2010) 2096–2103. https://doi.org/10.1016/j.fuel.2010.02.030.

[14] J. Osorio, F. Chejne, Bio-Oil Production in Fluidized Bed Reactor at Pilot Plant from Sugarcane Bagasse by Catalytic Fast Pyrolysis, Waste and Biomass Valorization. 10 (2017) 1–9. https://doi.org/10.1007/s12649-017-0025-8.

[15] Q. Lu, Z.-F. Zhang, C.-Q. Dong, X.-F. Zhu, Catalytic Upgrading of Biomass Fast Pyrolysis Vapors with Nano Metal Oxides: An Analytical Py-GC/MS Study, Energies. 3 (2010) 1805–1820. https://doi.org/10.3390/en3111805.

[16] H. Zhang, R. Xiao, H. Huang, G. Xiao, Comparison of non-catalytic and catalytic fast pyrolysis of corncob in a fluidized bed reactor, Bioresour. Technol. 100 (2009) 1428–1434. https://doi.org/10.1016/j.biortech.2008.08.031.

[17] K. Raveendran, A. Ganesh, K.C. Khilar, Influence of mineral matter on biomass pyrolysis characteristics, Fuel. 74 (1995) 1812–1822. https://doi.org/10.1016/0016-2361(95)80013-8.

[18] A.S. Amarasekara, C.C. Ebede, Zinc chloride mediated degradation of cellulose at 200 °C and identification of the products, Bioresour. Technol. 100 (2009) 5301–5304. https://doi.org/10.1016/j.biortech.2008.12.066.

[19] N. Shimada, H. Kawamoto, S. Saka, Different action of alkali/alkaline earth metal chlorides on cellulose pyrolysis, J. Anal. Appl. Pyrolysis. 81 (2008) 80–87. https://doi.org/10.1016/j.jaap.2007.09.005.

[20] J. Rizkiana, G. Guan, W.B. Widayatno, X. Hao, Z. Wang, Z. Zhang, A. Abudula, Oil production from mild pyrolysis of low-rank coal in molten salts media, Appl. Energy. 154 (2015) 944–950. https://doi.org/10.1016/j.apenergy.2015.05.092.

[21] H. S. Nygård, E. Olsen, Molten salt pyrolysis of milled beech wood using an electrostatic precipitator for oil collection, AIMS Energy. 3 (2015) 284–296. https://doi.org/10.3934/energy.2015.3.284.

[22] C. Shen, X. Jia, Y. Chen, L. Lu, F. Wang, Y. Wei, F. Yu, Molten carbonate pyrolysis of digestate with metal-modified HZSM-5 for bio-based monophenols: Kinetics and mechanism study, J. Anal. Appl. Pyrolysis. 151 (2020). https://doi.org/10.1016/j.jaap.2020.104929.

[23] S. Yoshida, J. Matsunami, Y. Hosokawa, O. Yokota, Y. Tamaura, M. Kitamura, Coal/CO2 gasification system using molten carbonate salt for solar/fossil energy hybridization, Energy and Fuels. 13 (1999) 961–964. https://doi.org/10.1021/ef980144n.

[24] R. and D.J.P. Datta, J.P. Dittami, J.P. Datta, Ravindra and Dittami, J.P. Dittami, Molten salt pyrolysis for bio-oil and chemicals, WO2017007798, 2016.

[25] H. Jiang, N. Ai, M. Wang, D. Ji, J. Ji, A. Ji, Experimental study on thermal pyrolysis of biomass in molten salt media, Electrochemistry. 77 (2009) 730–735. https://doi.org/10.5796/electrochemistry.77.730.

[26] M. Kudsy, H. Kumazawa, Pyrolysis of Krafi Lignin in the Presence of Molten ZnCl,-KCl Mixture, Can. J. Chem. Eng. 77 (1999) 1176–1184. https://doi.org/10.1002/cjce.5450770614.

[27] H.S. Nygård, F. Danielsen, E. Olsen, Thermal history of wood particles in molten salt pyrolysis, Energy and Fuels. 26 (2012) 6419–6425. https://doi.org/10.1021/ef301121j.

[28] H.S. Nygård, E. Olsen, Effect of Salt Composition and Temperature on the Thermal Behavior of Beech Wood in Molten Salt Pyrolysis, in: Energy Procedia, Elsevier, 2014: pp. 221–228. https://doi.org/10.1016/j.egypro.2014.10.432.

[29] P. Bhaumik, H.J. Chou, L.C. Lee, P.W. Chung, Chemical Transformation for 5-Hydroxymethylfurfural Production from Saccharides Using Molten Salt System, ACS Sustain. Chem. Eng. 6 (2018) 5712–5717. https://doi.org/10.1021/acssuschemeng.7b04815.

[30] P.-W. Chung, P. Bhaumik, C. Hao-Ju, Molten salt system and method and apparatus of transformation for multi-carbon production by using the same, (2020). https://worldwide.espacenet.com/patent/search/family/074090900/publication/TW202035382A?q=pn%3DTWI714035B.

[31] Y. Yang, H. Hu, F. Yang, H. Tang, H. Liu, B. Yi, X. Li, H. Yao, Thermochemical conversion of lignocellulosic bio-waste via fast pyrolysis in molten salts, Fuel. 278 (2020). https://doi.org/10.1016/j.fuel.2020.118228.

[32] D. Ji, M. Gao, F. Yu, N. Ai, H. Jiang, J. Ji, P. Yu, Conversion of sawdust to bio-fuels by pyrolysis within molten sodium hydroxide, in: Proc. 2012 Int. Conf. Biobase Mater. Sci. Eng. BMSE 2012, 2012: pp. 212–216. https://doi.org/10.1109/BMSE.2012.6466214.

[33] W. Deng, H. Jiang, Y. Wu, H. Fan, J. Ji, Hydrogen Production from Biomass Pyrolysis in Molten Alkali, AASRI Procedia. 3 (2012) 217–223. https://doi.org/10.1016/j.aasri.2012.11.036.

[34] G.E. Bertolini, J. Fontaine, Value recovery from plastics waste by pyrolysis in molten salts, Conserv. Recycl. 10 (1987) 331–343. https://doi.org/10.1016/0361-3658(87)90064-6.

[35] D. Serrano, A. Horvat, C. Sobrino, S. Sánchez-Delgado, Thermochemical conversion of C. cardunculus L. in nitrate molten salts, Appl. Therm. Eng. 148 (2019) 136–146. https://doi.org/10.1016/j.applthermaleng.2018.11.047.

[36] S. He, H.J. Heeres, J. Osorio Velasco, Laboratory gram-scale pyrolysis reactor, P35221PC00, 2023.

[37] J. Osorio Velasco, P. Badr, B. Sridharan, H. van de Bovenkamp, S. He, R.H. Venderbosch, H.J. Heeres, A novel staged free-fall reactor for pyrolysis and ex-situ catalytic pyrolysis of lignocellulosic biomass, unpublished work (2023).

[38] H.C. Genuino, L. Contucci, J.O. Velasco, B. Sridharan, E. Wilbers, O. Akin, J.G.M. Winkelman, R.H. Venderbosch, H.J. Heeres, Pyrolysis of LignoBoost lignin in ZnCl2-KCl-NaCl molten salt media: Insights into process-pyrolysis oil yield and composition relations, J. Anal. Appl. Pyrolysis. 172 (2023) 106005. https://doi.org/10.1016/J.JAAP.2023.106005.

[39] A. Estrada Leon, M. Pala, H.J. Heeres, W. Prins, F. Ronsse, Micro-pyrolysis of various lignocellulosic biomasses in molten chloride salts, J. Anal. Appl. Pyrolysis. 168 (2022) 105739. https://doi.org/10.1016/j.jaap.2022.105739.

[40] B. Sridharan, H.C. Genuino, D. Jardan, E. Wilbers, H.H. Van De Bovenkamp, J.G.M. Winkelman, R.H. Venderbosch, H.J. Heeres, Novel Route to Produce Hydrocarbons from Woody Biomass Using Molten Salts, (2022). https://doi.org/10.1021/acs.energyfuels.2c02044.

3.6. Supporting information – Chapter 3

Benchmark wood pyrolysis experiment in molten salts

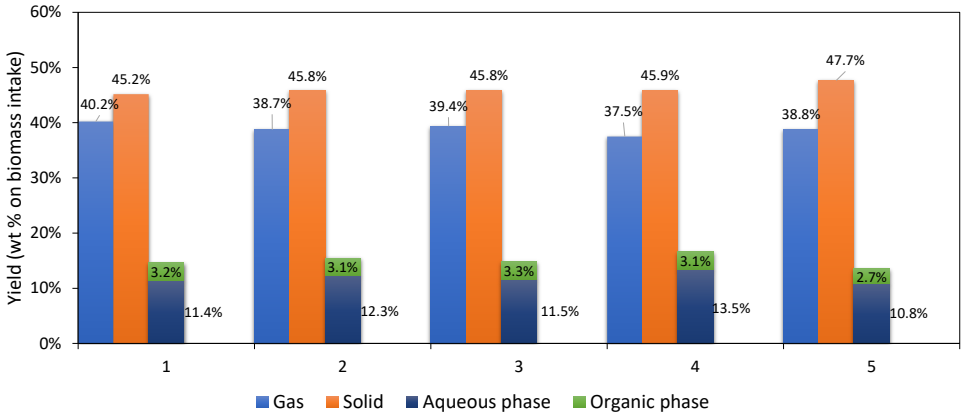

Figure S3.1. Benchmark pyrolysis experiment in molten salts at 375 °C and 45 wt % biomass in the feed.

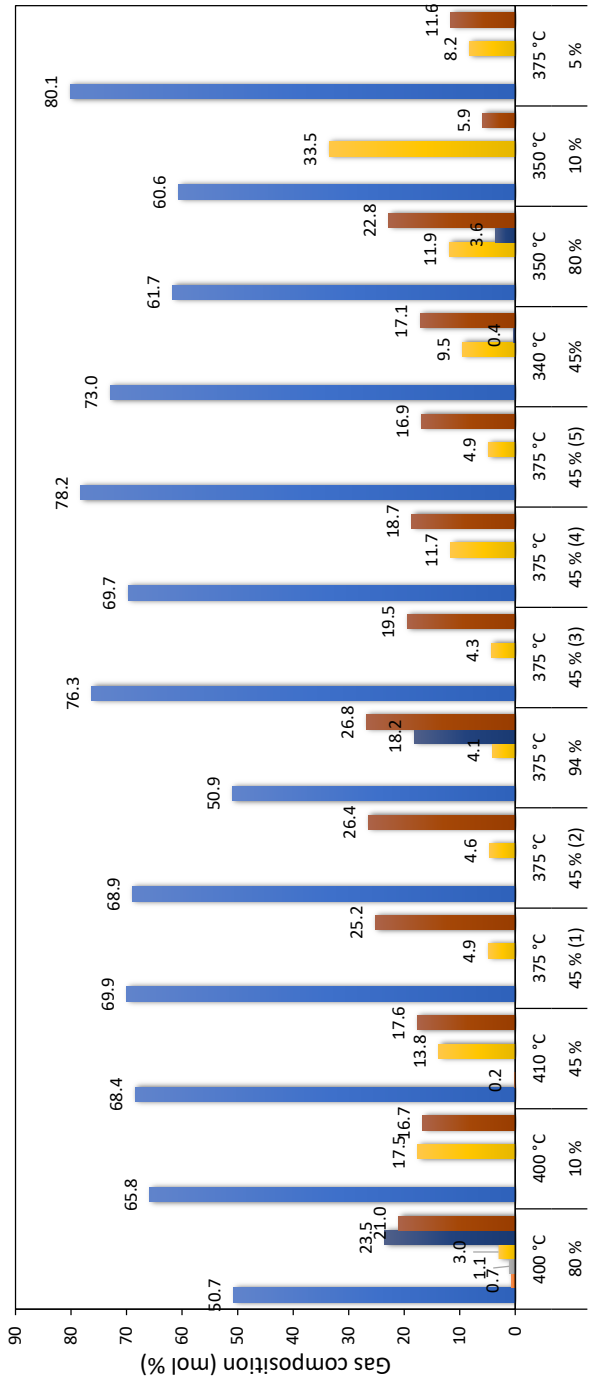

Figure S3.2. Gas composition for most of the experiments versus temperature and wt % of biomass in the feed.

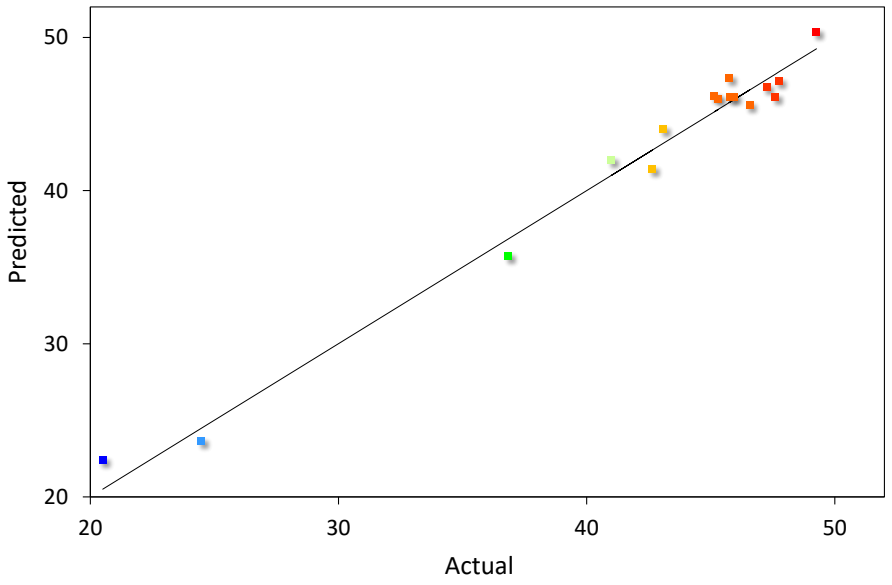

Figure S3.3. Parity plot for the char yield (wt % on biomass feed).

Table S3.1. ANOVA model summary for the liquid yield.

ANOVA for Response Surface Reduced Cubic Model

Analysis of variance table [Partial sum of squares - Type III]

Source	Sum of Squares	df	Mean Square	F Value	p-value Prob > F	
Model	3608.06	6	601.34	49.53	< 0.0001	significant
A-Temperature	*31.97*	*1*	*31.97*	*2.63*	*0.1357*	
B-biomass in th	*491.02*	*1*	*491.02*	*40.44*	*< 0.0001*	
AB	*13.18*	*1*	*13.18*	*1.09*	*0.3220*	
A^2	*34.07*	*1*	*34.07*	*2.81*	*0.1249*	
B^2	*3167.32*	*1*	*3167.32*	*260.86*	*< 0.0001*	
A^2B	*410.03*	*1*	*410.03*	*33.77*	*0.0002*	
Residual	121.42	10	12.14			
Lack of Fit	*116.20*	*6*	*19.37*	*14.85*	*0.0105*	*significant*
Pure Error	*5.22*	*4*	*1.30*			
Cor Total	3729.48	16				

Final Equation in Terms of Coded Factors:

Liquid yield =
+13.36
+2.46 * A
-15.64 * B
+3.04 * A * B
+4.41 * A^2
+38.78 * B^2
+37.37 * A^2 * B

Final Equation in Terms of Actual Factors:

Liquid yield =
-4177.55554
+22.72682 * Temperature
+93.37949 * biomass in the feed
-0.51219 * Temperature * biomass in the feed
-0.030338 * Temperature^2
+0.019584 * biomass in the feed^2
+6.85531E-004 * Temperature^2 * biomass in the feed

The Diagnostics Case Statistics Report has been moved to the Diagnostics Node.
In the Diagnostics Node, Select Case Statistics from the View Menu.

Proceed to Diagnostic Plots (the next icon in progression). Be sure to look at the:
1) Normal probability plot of the studentized residuals to check for normality of residuals.
2) Studentized residuals versus predicted values to check for constant error.
3) Externally Studentized Residuals to look for outliers, i.e., influential values.
4) Box-Cox plot for power transformations.

Table S3.2. ANOVA model summary for the liquid organic yield.

ANOVA for Response Surface Reduced Cubic Model

Analysis of variance table [Partial sum of squares - Type III]

Source	Sum of Squares	df	Mean Square	F Value	p-value Prob > F	
Model	395.29	7	56.47	122.63	< 0.0001	significant
A-Temperature	*9.18*	*1*	*9.18*	*19.94*	*0.0016*	
B-biomass in th	*27.48*	*1*	*27.48*	*59.68*	*< 0.0001*	
AB	*0.71*	*1*	*0.71*	*1.53*	*0.2467*	
A^2	*0.10*	*1*	*0.10*	*0.22*	*0.6514*	
B^2	*43.49*	*1*	*43.49*	*94.45*	*< 0.0001*	
A^2B	*7.85*	*1*	*7.85*	*17.04*	*0.0026*	
B^3	*11.69*	*1*	*11.69*	*25.39*	*0.0007*	
Residual	4.14	9	0.46			
Lack of Fit	*3.93*	*5*	*0.79*	*14.66*	*0.0111*	*significant*
Pure Error	*0.21*	*4*	*0.054*			
Cor Total	399.44	16				

Final Equation in Terms of Coded Factors:

Liquid organics yield =
+5.14
+1.35 * A
+19.76 * B
+0.73 * A * B
-0.30 * A^2
+6.29 * B^2
-10.25 * A^2 * B
-12.56 * B^3

Final Equation in Terms of Actual Factors:

Liquid organics yield =
+1276.67839
-6.78041 * Temperature
-27.54104 * biomass in the feed
+0.14152 * Temperature * biomass in the feed
+9.06105E-003 * $Temperature^2$
+0.024348 * biomass in the $feed^2$
-1.88066E-004 * $Temperature^2$ * biomass in the feed
-1.42583E-004 * biomass in the $feed^3$

The Diagnostics Case Statistics Report has been moved to the Diagnostics Node.
In the Diagnostics Node, Select Case Statistics from the View Menu.

Table S3.3. ANOVA model summary for the char yield.

ANOVA for Response Surface Reduced Cubic Model

Analysis of variance table [Partial sum of squares - Type III]

Source	Sum of Squares	df	Mean Square	F Value	p-value Prob > F	
Model	1023.25	7	146.18	72.63	< 0.0001	significant
A-Temperature	*4.76*	*1*	*4.76*	*2.37*	*0.1585*	
B-biomass in th	*2.362E-003*	*1*	*2.362E-003*	*1.173E-003*	*0.9734*	
AB	*1.90*	*1*	*1.90*	*0.95*	*0.3564*	
A^2	*13.36*	*1*	*13.36*	*6.64*	*0.0299*	
B^2	*390.52*	*1*	*390.52*	*194.02*	*< 0.0001*	
AB^2	*27.45*	*1*	*27.45*	*13.64*	*0.0050*	
B^3	*27.60*	*1*	*27.60*	*13.71*	*0.0049*	
Residual	18.11	9	2.01			
Lack of Fit	*14.64*	*5*	*2.93*	*3.37*	*0.1313*	*not significant*
Pure Error	*3.48*	*4*	*0.87*			
Cor Total	1041.36	16				

Final Equation in Terms of Coded Factors:

Char yield =
+46.18
-1.26 * A
+0.072 * B
+1.25 * A * B
+2.76 * A^2
-14.09 * B^2
-7.77 * A * B^2
+9.74 * B^3

Final Equation in Terms of Actual Factors:

Char yield =
+463.07905
-2.03795 * Temperature
-2.94547 * biomass in the feed
+0.011905 * Temperature * biomass in the feed
+2.25002E-003 * Temperature^2
+0.018528 * biomass in the feed^2
-1.12168E-004 * Temperature * biomass in the feed^2
+1.10562E-004 * biomass in the feed^3

The Diagnostics Case Statistics Report has been moved to the Diagnostics Node.
In the Diagnostics Node, Select Case Statistics from the View Menu.

Table S3.4. List of compounds in the pyrolysis liquid from the pyrolysis of sawdust with 100% biomass in the feed, 400 °C, solid residence time of 20 min, sample preheated at 100 °C for 5 min, N_2 flow at 17 ml min^{-1}.

Compound name	**Normalized peak intensity**
Acetic acid	0.80%
Acetaldehyde, hydroxy-	2.80%
Furan, tetrahydro- (solvent)	76.60%
2-Propanone, 1-hydroxy-	8.20%
Furan, tetrahydro-2-methyl-	0.40%
Furfural	0.90%
2-Furanmethanol	0.30%
2(5H)-Furanone	0.60%
2-Furancarboxaldehyde, 5-methyl-	0.20%
2-Cyclopenten-1-one, 2-hydroxy-3-methyl-	0.70%
Phenol, 2-methoxy-	1.10%
Phenol, 2-methoxy-4-methyl-	1.40%
1,2-Benzenediol	0.70%
1,4:3,6-Dianhydro-.alpha.-d-glucopyranose	0.30%
2,3-Anhydro-d-mannosan	0.20%
2-Furancarboxaldehyde, 5-(hydroxymethyl)-	0.20%
Phenol, 4-ethyl-2-methoxy-	0.50%
1,2-Benzenediol, 4-methyl-	0.20%
Eugenol	0.20%
Vanillin	0.20%
Phenol, 2-methoxy-4-(1-propenyl)-, (Z)-	0.60%
Butylated Hydroxytoluene (stabilizer in solvent)	1.50%
D-Allose	1.70%

Table S3.5. List of compounds in the pyrolysis liquid from the pyrolysis of sawdust with; 60 % of biomass in the feed, 400 °C, solid residence time of 20 min, sample preheated at 210 °C for 10 min, N_2 flow of 17 ml min^{-1}.

Compound name	**Normalized peak intensity**
Acetic acid	0.9%
Furan, tetrahydro- (solvent)	96.7%
Furfural	1.2%
Butylated Hydroxytoluene (stabilizer in solvent)	1.2%